Behavioral/Cognitive

The Influence of Prestimulus 1/f-Like versus Alpha-Band Activity on Subjective Awareness of Auditory and Visual Stimuli

Emily Cunningham,[1,2] **Clementine Zimnicki,**[1] **and Diane M. Beck**[1,2]

[1]Department of Psychology, University of Illinois Urbana-Champaign, Champaign, Illinois 61820 and [2]Beckman Institute for Advanced Science and Technology, University of Illinois Urbana-Champaign, Urbana, Illinois 61801

Alpha rhythmic activity is often suggested to exert an inhibitory influence on information processing. However, relatively little is known about how reported alpha-related effects are influenced by a potential confounding element of the neural signal, power-law scaling. In the current study, we systematically examine the effect of accounting for 1/f activity on the relation between prestimulus alpha power and human behavior during both auditory and visual detection ($N = 27$; 19 female, 6 male, 2 nonbinary). The results suggest that, at least in the scalp-recorded EEG signal, the difference in alpha power often reported before visual hits versus misses is probably best thought of as a combination of narrowband alpha and broadband shifts. That is, changes in broadband parameters (exponent and offset of 1/f-like activity) also appear to be strong predictors of the subsequent awareness of visual stimuli. Neither changes in posterior alpha power nor changes in 1/f-like activity reliably predicted detection of auditory stimuli. These results appear consistent with suggestions that broadband changes in the scalp-recorded EEG signal may account for a portion of prior results linking alpha band dynamics to visuospatial attention and behavior, and suggest that systematic re-examination of existing data may be warranted.

Key words: **alpha; auditory; awareness; EEG; oscillation; visual**

Significance Statement

Fluctuations in alpha band (~8–12 Hz) activity systematically follow the allocation of attention across space and sensory modality. Increases in alpha amplitude, which often precede failures to report awareness of threshold visual stimuli, are suggested to exert an inhibitory influence on information processing. However, fluctuations in alpha activity are often confounded with changes in the broadband 1/f-like pattern of the neural signal. When both factors are considered, we find that changes in broadband activity are as effective as narrowband alpha activity as predictors of subsequent visual detection. These results are consistent with emerging understanding of the potential functional importance of broadband changes in the neural signal and may have significant consequences for our understanding of alpha rhythmic activity.

Introduction

The amplitude of alpha rhythmic activity (~8–12 Hz), a prominent feature of the scalp-recorded EEG signal, fluctuates systematically in response to attentional demands. When attention is allocated spatially, for example, posterior alpha power tends to decrease contralateral to the attended location relative to ipsilateral to it (Worden et al., 2000; Thut et al., 2006, among many others). In addition to attention-induced shifts in signal distribution, numerous reports link amplitude of ongoing posterior alpha activity to behavior, particularly the subjective awareness of near-threshold stimuli (Ergenoglu et al., 2004; Limbach and Corballis, 2016; Iemi et al., 2017; Samaha et al., 2017; for a review, see Samaha et al., 2020). When taken together with intracranial reports linking reduced neuronal firing to increased alpha amplitude (Haegens et al., 2011), the modal view is that patterns of attentional alpha power increase may reflect functional inhibition of information processing.

However, interpretation of existing alpha-related phenomena is complicated by another ubiquitous feature in recordings of neuronal activity, power-law (1/f) scaling (Miller et al., 2009). Shifts in this broadband pattern can masquerade as changes in alpha activity and are easily confounded with alpha amplitude when activity is reported in the conventional manner. Notably,

Received Jan. 24, 2023; revised Aug. 1, 2023; accepted Aug. 2, 2023.

Author contributions: E.C., C.Z., and D.M.B. designed research; E.C. and C.Z. performed research; E.C. and C.Z. analyzed data; and E.C. wrote the paper.

This work was supported by a Beckman Institute for Advanced Science and Technology fellowship to E.C. and a research award to C.Z. We thank Gabriele Gratton for feedback provided on an earlier version of this manuscript and Andrew Severs and Dajana Duci for help with data collection.

C. Zimnicki's present address: Department of Psychology, University of Wisconsin-Madison.

The authors declare no competing financial interests.

Correspondence should be addressed to Emily Cunningham at ecnnngh2@illinois.edu.

https://doi.org/10.1523/JNEUROSCI.0238-23.2023

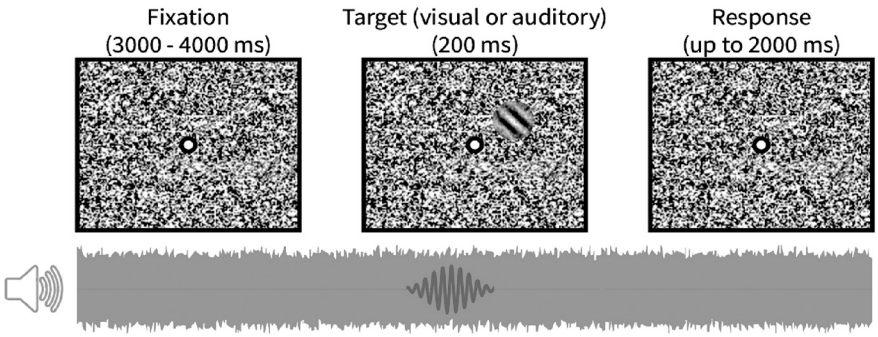

Figure 1. Illustration of a visual/auditory trial. In the visual case, only the Gabor target was presented. In the auditory case, only the tone was presented.

changes in broadband spectral features have been linked to changes in excitation–inhibition balance that are also likely to be associated with attentional shifts and behavioral outcomes (Gao et al., 2017). For example, broadband slope and offset change dynamically in response to visual stimulation (Podvalny et al., 2015; Gyurkovics et al., 2022) and relate to cognitive variables in ways that may account for variation that would otherwise be considered alpha related (Ouyang et al., 2020). Systematic examinations of the relation between narrowband alpha activity and broadband shifts have not been performed until relatively recently (Podvalny et al., 2015; Donoghue et al., 2020a; Iemi et al., 2019; Ouyang et al., 2020; Waschke et al., 2021; Gyurkovics et al., 2022; Iemi et al., 2022), and the extent to which previously reported effects should be considered truly (or specifically) alpha related is unclear.

The data presented here derive from an experiment designed to examine the relation between posterior alpha power and subjective awareness when attention is directed to auditory relative to visual information, building on a growing interest in the extension of alpha-related dynamics across modalities. In brief, although most examinations of alpha activity involve manipulations of attention within a single modality (usually vision), posterior alpha signals are also predictably modulated by intersensory demands. For example, when participants are cued to attend to auditory information, alpha power over parieto-occipital regions increases relative to cues to attend to vision (Adrian, 1944; Foxe et al., 1998; Fu et al., 2001; Mazaheri et al., 2014; van Diepen and Mazaheri, 2017). These posterior alpha increases tend to be interpreted as effects of visual suppression when attention is directed to the auditory modality. However, it is not clear if/when changes in alpha amplitude over visual areas should impact the processing of attended auditory information. Although several suggestive reports link greater parieto-occipital alpha power to improved responses to auditory information (Makeig and Inlow, 1993; Bollimunta et al., 2008; Elshafei et al., 2018; see also Haegens et al., 2012), there are at least as many mixed, negative, or opposing reports (Bernasconi et al., 2011; Ng et al., 2012; Mazaheri et al., 2014; Strauß et al., 2015; Kayser et al., 2016; van Diepen and Mazaheri, 2017; Hansen et al., 2019).

As might be expected, these discussions are complicated by analytic techniques that confound broadband changes in EEG/MEG signals with narrowband shifts in oscillatory activity (Donoghue et al., 2020a). The purpose of this work was to systematically evaluate the relation between prestimulus alpha activity, 1/f scaling, and behavior in the context of audition and vision, taking advantage of a dataset in which participants completed challenging auditory and visual detection tasks in separate sessions with eyes open.

Materials and Methods

Participants

The relation between prestimulus alpha power and visual detection can be observed with as few as 8–12 participants (Ergenoglu et al., 2004; Busch et al., 2009; Mathewson et al., 2009; MEG, Dijk et al., 2008). Similarly, differences in amplitude of the alpha signal following cues to attend to auditory relative to visual information are readily observed in sample sizes of 9–18 (EEG, Foxe et al., 1998; Fu et al., 2001; MEG, Mazaheri et al., 2014). Available information on the association between alpha power and auditory detection is comparatively limited, but existing mixed reports typically come from sample sizes of <15 (Bernasconi et al., 2011; Ng et al., 2012; Strauß et al., 2015; Kayser et al., 2016; Hansen et al., 2019). Given this information, the target sample size was initially set to 30 (roughly double the power of most existing reports in this domain).

Data collection was interrupted because of the COVID-19 pandemic with data from 15 participants. A portion of this data was analyzed for a bachelor thesis before in-person research resumed. Given this examination, and considering time lost to pandemic-related precautions, the initial sampling protocol was adapted to implement a descriptive approach with a precision-based stopping rule based on confidence interval width, such that the minimum number of additional participants was run to obtain estimates of alpha-related effects with the desired level of precision. To that end, data collection continued until either the initial target sample size of 30 was achieved, or the following criteria were met: (1) For $\text{visual}_{\text{hit-miss}}$ and $\text{auditory}_{\text{hit-miss}}$ contrasts, the average width (over the six parietal/occipital electrode sites) of the 95% bootstrapped confidence intervals of the difference in average log-transformed power (before adjustment for aperiodic fits) should be ≤ 0.10 $\log(\mu V^2)$, and (2) for the contrast '$\text{visual}_{\text{hit-miss}}$ versus $\text{auditory}_{\text{hit-miss}}$', as well as for $\text{hit}_{\text{auditory-visual}}$ contrasts, the mean width of 95% bootstrapped CIs should be ≤ 0.15 log (μV^2) over the same set of electrodes.

These conditions were met after data were obtained from 27 participants (age 18–27 years; 19 female, 6 male, 2 nonbinary). Four additional participants completed the study but failed to meet inclusion criteria (see below, Data analysis). All participants reported normal or corrected-to-normal vision and hearing, along with no history of epilepsy or psychiatric disorder. Participants were compensated at a rate of $8/h. All participants gave written informed consent before participation, and all procedures were approved by the Institutional Review Board at the University of Illinois Urbana-Champaign.

Experimental design and statistical analysis

Visual targets consisted of Gabor patches that were 3.25° in diameter with a spatial frequency of 1.54 cycles/degree. Targets were oriented 135° clockwise from vertical and presented 1.94° above and 2.43° to either the left or right (with equal probability) of a white fixation dot in the center of the display. Auditory targets were Hamming-windowed 500 Hz tones delivered to either the left or right speaker (also with equal probability). Visual and auditory targets were embedded in a constant background of visual and auditory white noise (Fig. 1; for visual white noise, grayscale pixel values were drawn from a uniform distribution ranging from black

to white). This background was identical across tasks, such that the only difference between the tasks was the modality of target presentation.

Each trial began with a jittered 3000–4000 ms blank interval followed by a 200 ms target. Participants responded with a right-hand key press whenever a target was detected. Responses were considered successful detection if they occurred within a 2000 ms window following target onset. Subsequent trials began either immediately following a response or after 2000 ms if no response was provided. On 20% of trials, no target was presented. As participants were not provided with any indication of the beginning or end of a trial and were not required to make target-absent responses, target-absent trials appeared to them as blank periods of 5200–6200 ms.

Auditory and visual tasks were completed in separate sessions spaced at least 24 h and at most 2 weeks apart, with order counterbalanced across participants. Before each task, participants completed a brief practice session consisting of low-difficulty targets (high amplitude or high contrast) with feedback. This session was repeated until participants achieved at least 80% accuracy. Following the practice period, the discriminability of auditory and visual targets from the white noise background was adjusted over 60 trials of an adaptive three-down-one-up staircase targeting a detection rate of 80% (with step size of the change in contrast/volume decreasing over trials). On visual trials, Gabor patches were adjusted by changing the greyscale value of each pixel relative to the background, adjusting the apparent opacity of the stimulus. On auditory trials, the amplitude of targets was adjusted relative to the white noise background.

Each task was divided into 12 blocks of 52 trials (624 trials per session) with self-paced breaks between blocks. In each block, the stimulus was present for 42 trials and absent for 10 trials. To minimize criterion shifts throughout the session, the first two trials of each block served as reference trials (target-present trials in which the contrast/volume of the stimulus was increased slightly above threshold). For both visual and auditory tasks, participants were instructed to keep their eyes open and fixated on the fixation dot and were monitored for compliance.

Participants were seated in an unshielded room with the lights off, and viewing distance was constrained with a chin rest to 63 cm. Visual stimuli were presented using an 18 inch CRT monitor with a refresh rate of 85 Hz and a resolution of 1024 × 768. The experiment was programmed in Python (version 3.6) using the Psychopy library (version 3.2.4; Peirce et al., 2019) on a computer running Ubuntu 16.04 LTS. Auditory stimuli were presented through Dell model A215 speakers, which were positioned 41 cm to the left and right of the center of the display. The auditory white noise background was set at an intensity of ~57 dB. On reinitiating the experiment following the pandemic shutdown, an emergent fault was discovered in the initial speaker setup in which stimuli presented over the left speaker were slightly louder than stimuli presented through the right speaker (a difference of ~1 dB). Once the issue was detected, the speakers were replaced. Where relevant, auditory data are separated into those affected ($n = 15$) and unaffected ($n = 12$) to identify effects attributable to speaker malfunction.

Data acquisition

EEG was recorded from 12 Ag/AgCl electrodes positioned at Fz, T7, C3, Cz, C4, T8, P3, Pz, P4, O1, Oz, and O2 locations in a standard 10/20 array (EasyCap), using a 16-channel BrainVision V-Amp amplifier and BrainVision Recorder software (Brain Products). Electrodes were referenced online to FCz with a ground positioned at FPz. Electrodes placed at left and right mastoids were used for off-line rereferencing. EOG was recorded from electrodes placed above and below the left eye. All impedances were adjusted to <10 kΩ. EEG was digitized at 1 kHz with a 500 Hz low-pass anti-aliasing filter.

EEG preprocessing

EEG recordings were preprocessed in Python (version 3.10) using the MNE-Python library (version 0.24.1; Gramfort et al., 2013). Data were high-pass filtered off-line at 0.1 Hz (Hamming-windowed sinc filter, order 33,000), rereferenced to the average of left and right mastoid channels and epoched from −2000 to 1000 ms surrounding target onset. Blink artifacts were corrected using the regression technique described by Gratton et al. (1983). Trials containing voltage fluctuations exceeding 150 μV in channels C3, Cz, C4, P3, Pz, P4, O1, Oz, O_2 in the interval from −1000 to 0 ms were rejected. An average of 605 auditory trials and 602 visual trials were retained for each participant. Data were left and right reversed for trials in which stimuli were presented to the left of the participant to create a contralateral/ipsilateral organization (such that in plots, electrodes left of center are contralateral to the stimulus location).

For each trial, data were extracted over the 500 ms window immediately preceding stimulus onset. (In the literature on visual detection, this is the window over which prestimulus alpha power differences tend to be most pronounced.) The fast Fourier transform (zero padded to 2048 points, or a frequency resolution of ~0.5 Hz) was computed over the Hamming-windowed data. Resulting power spectral densities (PSDs) formed the primary units of analysis for the group-average and single-trial decompositions described below.

Data analysis

Data and code for this experiment can be found at https://osf.io/2u4g9/.

Exclusion criteria. Participants were excluded from analysis if they met any of the following criteria: (1) failing to produce at least 20 trials in each auditory/visual hit/miss category after data processing (Simulations based on pilot data suggest reliable estimates of unadjusted alpha power require at least 20 trials; $n = 2$ participants met this condition.), (2) poor data quality, as indexed by rejection of >25% of trials (No participants met this condition.), or (3) no identifiable alpha peak in either task for a majority of electrode locations, with identifiable defined as a peak in the range 6–14 Hz identified through the fitting procedure described below ($n = 2$ participants met this condition).

Spectral parameterization. Single-trial power spectra were averaged separately for each participant, electrode, task, and behavioral bin (hit/miss) and fed to an iterative fitting procedure that was used to parameterize the aperiodic and periodic components of the spectrum (specparam, formerly FOOOF, version 1.0.0; Donoghue et al., 2020a). This procedure assumes the PSD is composed of an aperiodic broadband component, here fitted as:

$$L(F) = b - \log(F^{\chi}),$$

where F refers to frequency, and b (offset) and χ (exponent) are free parameters, together with a variable number of potential periodic components modeled with Gaussians. Additional settings fed to the algorithm were peak width limits = [0.5, 6]; maximum number of peaks, 6; minimum peak height, 0.05; and peak threshold, 2. Power spectra were parameterized over the range 2–50 Hz. The average R^2 value over all fits was 0.99 (SD = 0.02). Split by task modality, the average R^2 value for auditory spectra was 0.99 (SD = 0.02), and the average R^2 value for visual spectra was 0.99 (SD = 0.03; the difference in R^2 between tasks averaged 0.002).

Alpha peak frequency (APF) was defined as the algorithmically identified peak in the range 6–14 Hz (Bazanova and Vernon, 2014; Haegens et al., 2014). Alpha power, before and after adjustment for aperiodic fit, was extracted as the area under the curve from APF − 2 Hz to APF + 2 Hz. Note that although aperiodic fits were computed in log space, adjustment was performed in linear space.

One of the purposes of the protocol described by Donoghue et al., (2020a) is to accurately parameterize spectra, limiting pitfalls associated with misinterpreting broadband effects or frequency shifts as shifts in oscillatory power. Peak frequencies are discovered every time the fit is performed, meaning that APF could in principle fluctuate for hits or misses and across channel and task. As identification of peaks using this algorithm is data driven and agnostic to expected frequency, there is also no guarantee that any given individual will have an identifiable alpha peak. (In fact, this is to be expected for some subset of participants, given that ~1 in 10 people have a very low-voltage or undetectable scalp-recorded alpha signal; Bazanova and Vernon, 2014). In addition, in this experimental context, it is expected that an alpha peak may be absent or greatly reduced in some conditions relative to others (e.g., for visual hits relative to misses). Participants with no identified α peak in a majority of

channels were excluded from analyses as outlined in the exclusion criteria above. However, when there was partial failure to identify alpha peaks (i.e., peaks were identified by the algorithm in some conditions but not others.), APF was assigned as the average of the alpha peak frequencies that were successfully identified for that participant/channel. This assignment was applied only for the purposes of deriving alpha power estimates.

Single-trial alpha power. To estimate single-trial alpha power, a single alpha center frequency estimate was identified for each individual/electrode based on the average of identified alpha peak frequencies over the set of four modality/behavioral bins. To obtain adjusted power values and estimates of aperiodic offset/exponent for each trial, PSDs for each trial/channel were fed to the fitting algorithm in the same manner as described above. Alpha power was quantified as the average of spectra from APF − 2 Hz to APF + 2 Hz both before and after adjusting for the aperiodic fit (in linear space). Aperiodic exponent and offset values were also saved for subsequent analyses.

As should be expected, single-trial fits were considerably noisier than fits to the average. The average R^2 value across all participants (after single-trial R^2 values were averaged over all tasks and channels within participant) was 0.72 (SD = 0.05, range = 0.58−0.80). Split by task modality, the average R^2 value for auditory trials was 0.72 (SD = 0.06), and the average R^2 value for visual trials was 0.72 (SD = 0.06; i.e., the difference in fit quality across tasks was minimal, $\text{mean}_{\text{difference}} = 0.001$.

Statistical analysis. Data were analyzed in R using tidyverse (Wickham et al., 2019), lme4 (Bates et al., 2015), sjPlot (https://CRAN.R-project.org/package=sjPlot), boot (https://CRAN.R-project.org/package=boot), ggdist (https://doi.org/10.5281/zenodo.6862765), data.table (https://CRAN.R-project.org/package=data.table), and patchwork (https://patchwork.data-imaginist.com/) packages. The analytic approach focused on description/estimation. Where contrasts across modality/behavioral bin are computed, averaged difference scores are provided as point estimates, together with associated 95% bootstrapped confidence intervals (computed using the percentile method) and standardized effect sizes (Cohen's d_z).

In the literature, contrasts across behavioral bins are often complemented by an additional analysis that reflects the hypothesis that alpha power predicts performance within individuals at the single-trial level. In most cases, trials are sorted by alpha power from low to high for each participant and grouped into 5–10 quantiles. Hit rate is then analyzed as a function of quantile, often by calculating differences between hit rates associated with the most extreme quantiles in the set. This analysis is effectively a simplification of a linear mixed-effects logistic regression approach.

Here, we produce these quantiles (in bins of five) to aid visualization but conduct mixed-effect logistic regression analyses on single-trial data of all participants separately for each channel and task modality. The mixed-effects approach allows for evaluation of the effects of predictors nested within a hierarchical structure, in this case, the effects of alpha band and aperiodic predictors on the log odds of a hit nested within the individual. Before model fitting, predictors were standardized within individual/task/channel to place them on similar scales and to aid interpretation of fixed effects in the final models (such that fixed effects can be interpreted in relation to a unit SD change in offset, exponent, or alpha power). Model fitting and interrogation were performed using the lme4 and sjPlot packages in R.

Model fits were evaluated by examining the extent to which a model including a fixed effect (and random slope, where indicated) for a given predictor provided a better fit relative to a null model including a random intercept for individual, with fit quality indexed by the Akaike information criterion (AIC; Akaike, 1974). Note that AIC values for a given set of models are meaningful only in a relative sense, with preference given to models with lower AIC estimates (i.e., of two models, the model with the lower AIC value is the model that minimizes information loss relative to an unknown ground truth for which both models are designed to account). In evaluating AIC values, there is no hard rule regarding a minimum difference of interest, but cautious guidelines suggest that at ΔAIC values of ≤ 2, evidence favoring one or the other model is equivocal, and that at ΔAIC values of ≥ 10, the model with the greater AIC value is comparatively implausible (Burnham et al., 2011).

Fit values were supplemented with reports of the fixed-effect estimates associated with adjusted and unadjusted power, offset, and exponent as well as 95% confidence intervals surrounding the fixed effects.

Results

Data collection proceeded until stopping criteria were met, resulting in a sample size of 27 (Average 95% $\text{CI}_{\text{difference}}$ widths for stopping-criteria contrasts were: $\text{visual}_{\text{hit-miss}} = 0.06$, $\text{auditory}_{\text{hit-miss}} = 0.07$, difference between $\text{visual}_{\text{hit-miss}}$ and $\text{auditory}_{\text{hit-miss}} = 0.09$, and $\text{hit}_{\text{aud-miss}} = 0.15$). An additional four participants were recruited but failed to meet inclusion criteria. (Two participants were excluded for having fewer than 20 trials in at least one auditory/visual hit/miss bin, and two participants were excluded for having no detectable alpha peak over more than half of the electrode sites; in one case, no alpha peak was identified for any combination of channel/task/behavior, and in the other case, an alpha peak was identified in only two channels, and in those channels, only for auditory hits).

Behavior

Detection tended to be better for auditory relative to visual targets, with hit rates in the auditory task averaging 0.74 (SD = 0.20) and hit rates in the visual task averaging 0.57 [SD = 0.12; $\text{mean}_{difference} = 0.17$, 95% $\text{CI}_{\text{difference}}$ (0.07, 0.25)]. False alarms were rare, with rates averaging 0.03 (SD = 0.09) in the visual task and 0.05 (SD = 0.05) in the auditory task. The effect of the speaker fault was apparent in the auditory data, such that participants experiencing the fault ($n = 15$) had higher hit rates for left-presented (mean = 0.89, SD = 0.20) than right-presented trials [mean = 0.60, SD = 0.27; $\text{mean}_{\text{L-}R} = 0.30$, 95% $\text{CI}_{\text{L-R}}$ (0.17, 0.42)]. After the issue was corrected, hit rates were approximately equivalent across target positions [left, mean = 0.74, SD = 0.26; right, mean = 0.73, SD = 0.21; $\text{mean}_{\text{L-}R} = 0.02$, 95% $\text{CI}_{\text{L-R}}$ (−0.06, 0.10)]. Given this discrepancy, all analyses involving auditory data were queried to determine whether there was evidence of an effect of speaker fault on the outcome (see above, Materials and Methods). Cases in which the conclusions drawn regarding an effect would differ before or after speaker replacement are discussed directly where relevant.

Aperiodic fits

Aperiodic fits and the effects of adjustment are illustrated in Figure 2 for a representative electrode. Offset and exponent estimates were evaluated independently (Fig. 3). As a reminder, greater offset values indicate a broadband translation (a higher projected intercept in log–log space), whereas greater exponent values translate to a steeper negative slope in the log–log power spectrum. Note that although offset and exponent are both presented here, these two parameters are often strongly correlated (just as slope and intercept both shift when a line is rotated around a point). Observing effects along both dimensions does not necessarily indicate independent variation in both components.

With respect to offset, visual misses were consistently associated with larger offsets than visual hits, with effects becoming quite pronounced over posterior electrodes (d_z values ranging from 0.79 to 1.37; Figs. 2*D*, 3*B*, right); otherwise, differences as a function of modality and behavior were small and inconsistent. Differences in exponent followed a similar pattern; differences were minimal for most comparisons, apart from the $\text{visual}_{\text{hit-miss}}$ contrast where they became quite pronounced toward the posterior (Figs. 2*E*, 3*D*). Over the occipital row, visual misses were consistently associated with larger exponent values than visual hits, with d_z values ranging from 0.56 to 1.00.

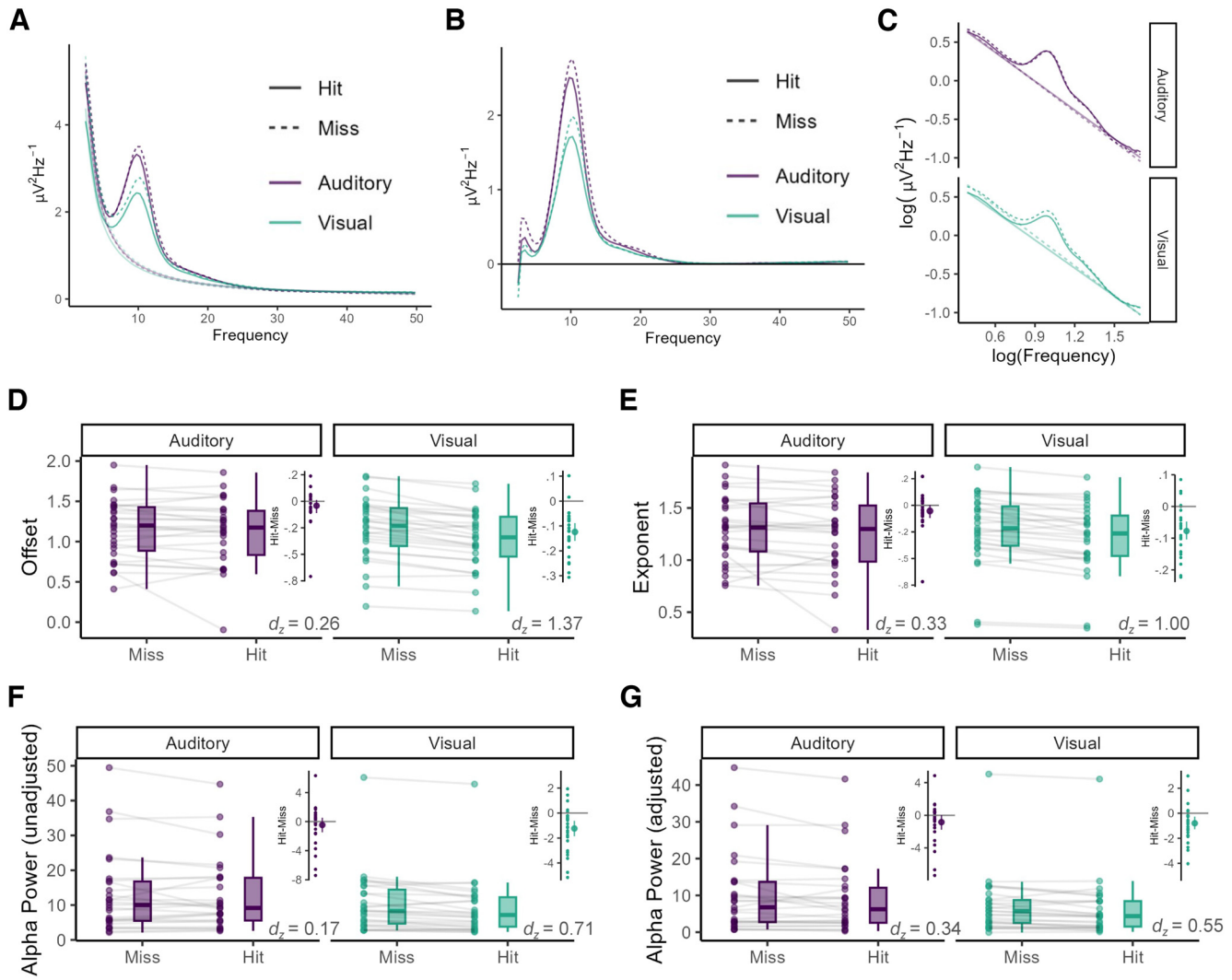

Figure 2. Aperiodic and alpha band components of the spectrum illustrated for a representative electrode (Oz). ***A***, Power spectra and associated aperiodic fits. ***B***, Spectra after subtraction of aperiodic component. ***C***, Spectra and aperiodic fits in log–log space, separated by task for ease of visualization (straight lines indicate aperiodic fits). ***D–G***, Offset, exponent, unadjusted alpha power, and adjusted alpha power at electrode Oz. Gray lines connect values from the same individual. Inset plots indicate differences between hits and misses. Visual (green) misses were consistently associated with larger alpha power, offset, and exponent than visual hits. The same comparisons for the auditory task (purple) did not yield consistent results. Oz was selected for this visualization (and that of Fig. 6) based on the data from Figures 3 and 4 and to facilitate comparison with visual data from previously published work. The auditory data do not appear substantially different when viewed from more central electrode locations (e.g., Cz), but the limited coverage of frontocentral sites here precludes strong statements about activity at locations typically associated with auditory processing.

Alpha power before and after adjustment for the aperiodic component of the spectrum

Before analyses of alpha power, the position and spread of alpha-band activity (in terms of alpha bandwidth and center frequency) were examined to ensure there were no differences across conditions (Donoghue et al., 2020a). Across channel, task, and behavioral bin (hit/miss), estimated alpha bandwidths were relatively consistent, averaging 3.67 Hz, with minor and unsystematic differences between auditory/visual and hit/miss conditions ranging in magnitude from 0.002 to 0.36 Hz. Differences in alpha peak frequency as a function of modality/behavior were similarly minor, with average differences across hit/miss and auditory/visual conditions ranging from 0.0002 to 0.51 Hz ($\text{mean}_{overall}$ = 10.02 Hz). Note that these analyses were carried out for the 24 participants with identifiable alpha peaks across all channels/bins. Among included participants, there were three participants for whom alpha peaks were not identified for some combinations of task/bin within a channel. For one participant, alpha peaks were not identified during the visual task over the three occipital electrode sites. For the second participant, no alpha peak was identified over parietal electrode sites during auditory hits and over occipital sites for a combination of visual misses and auditory hits/misses. In the third case, alpha peaks were not identified for a combination of central/occipital auditory hits/misses. In these participants, for alpha power estimation only (see above, Materials and Methods), alpha peak frequency for the missing conditions was assigned as the average peak frequency over the remaining bins for that electrode (e.g., if a participant had no identified alpha peak for auditory misses at channel Pz, alpha peak frequency would be assigned as the average of frequency estimates for visual hits, visual misses, and auditory hits at Pz).

To assess the extent to which changes in the aperiodic component of the signal had an impact on measurement of alpha power, power in the alpha band was computed both before and after fitting and removing the aperiodic component of the spectrum.

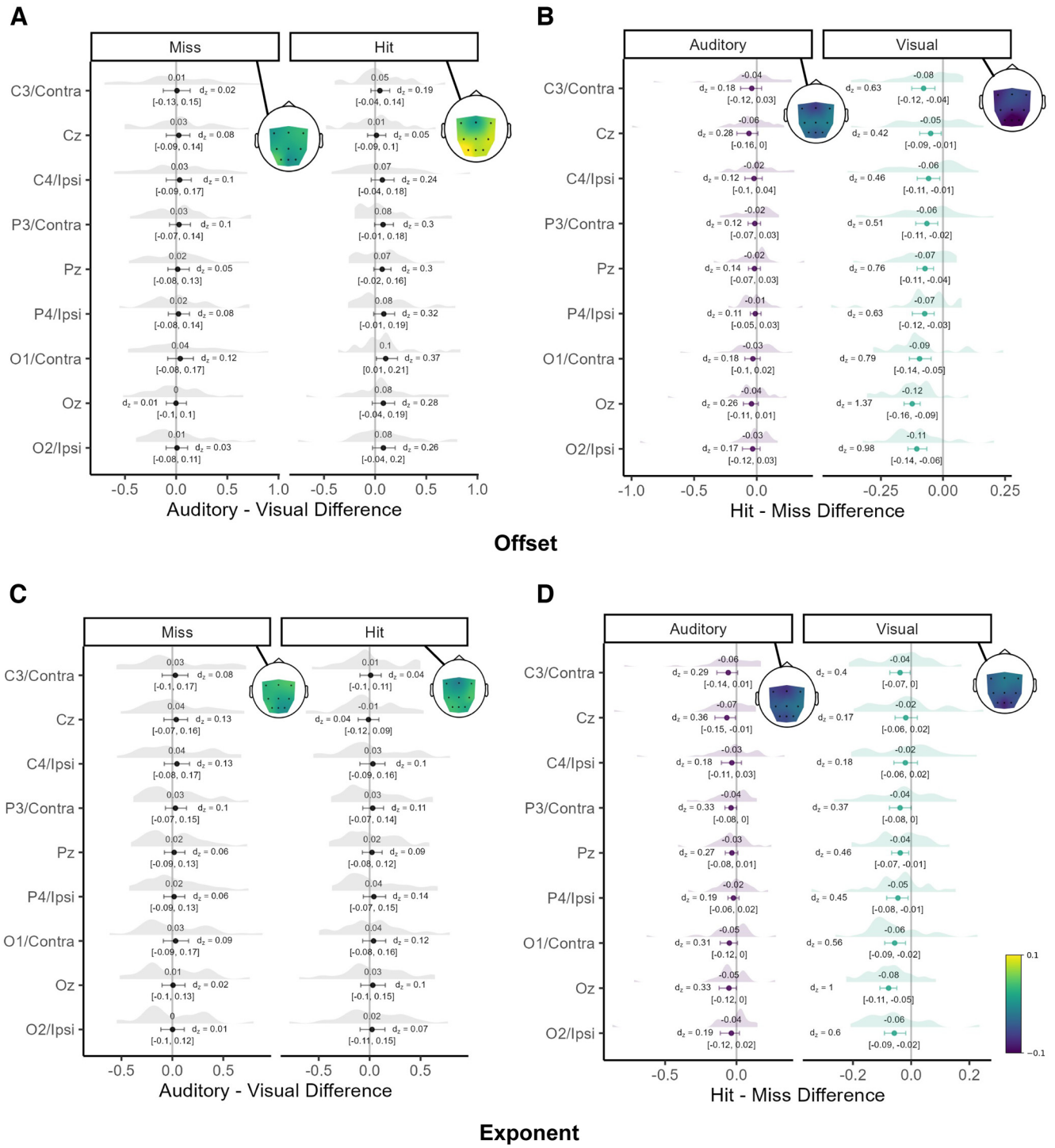

Figure 3. ***A***, Difference in offset before auditory versus visual hits (right) and misses (left) across nine electrode sites, arranged from anterior to posterior. Each point and the number above it indicate the mean difference across participants. Error bars and the interval estimate below indicate 95% bootstrapped CIs around the mean difference. Cohen's d_z effect size estimates are reported to the left/right of center for each electrode, with position reflecting the direction of the effect. Associated distributions of differences and topographic representations of mean differences are also plotted for each condition. ***B***, Difference in offset before auditory (left) and visual (right) hits and misses. ***C***, Difference in exponent before auditory versus visual hits (right) and misses (left). ***D***, Difference in exponent before auditory (left) and visual (right) hits versus misses.

Before aperiodic correction

Before adjusting for the aperiodic (1/f-like) component of the spectrum, and consistent with existing reports (Foxe et al., 1998; Fu et al., 2001; Mazaheri et al., 2014; van Diepen and Mazaheri, 2017), posterior alpha activity tended to be amplified when attending to auditory relative to visual information (Fig. 4*A*), even though auditory and visual data were recorded in separate sessions on separate days. This is broadly consistent with the notion that these relative changes in amplitude emerge automatically when attention is directed toward or away from vision, even when there is no expectation of transient extramodal competition (i.e., in the context of a static visual display). The magnitude of the difference was more pronounced for hits than misses (with d_z values ranging from 0.54 to 0.62 for hits and 0.39 to 0.5

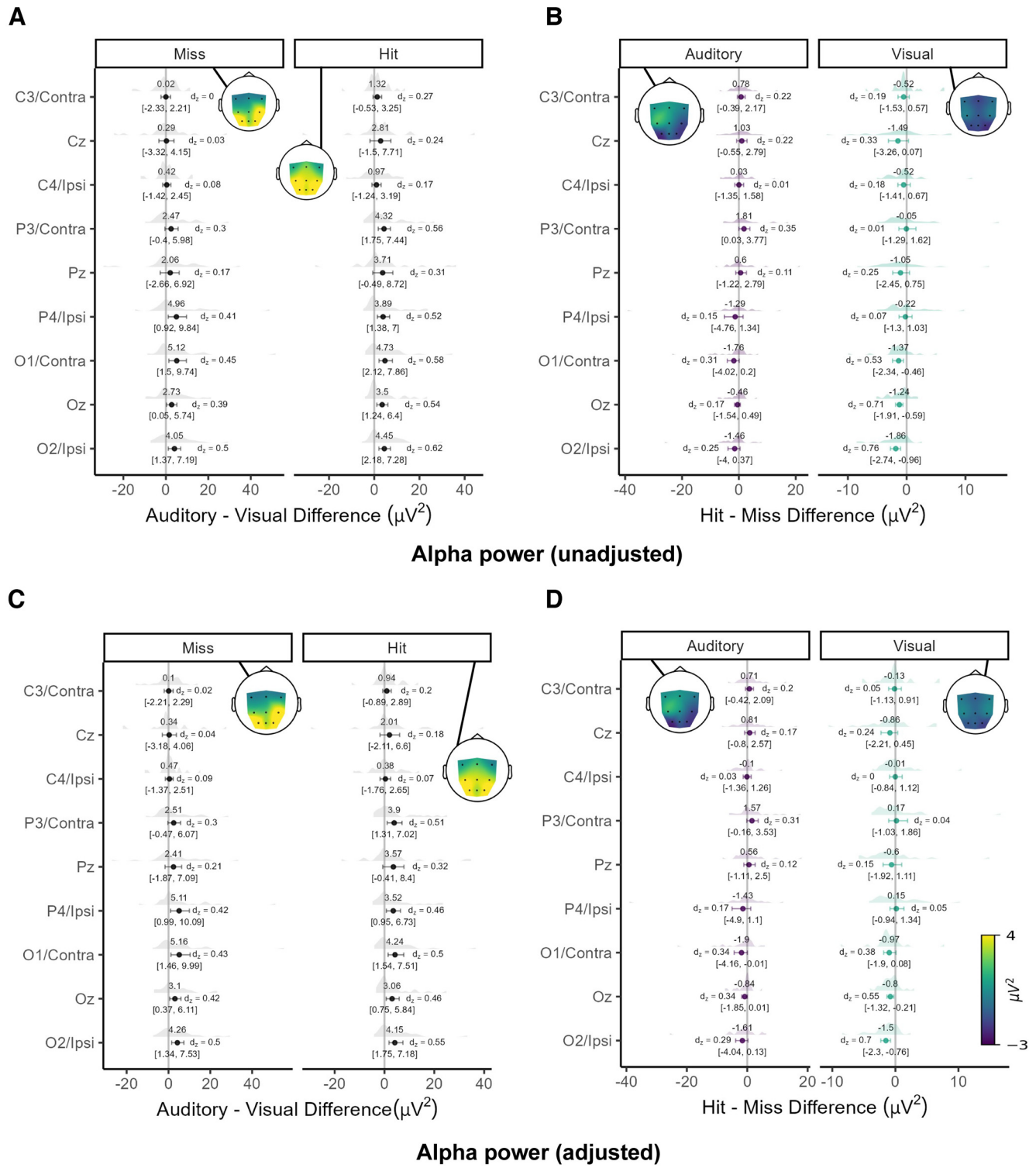

Figure 4. ***A***, Difference in unadjusted alpha power before auditory versus visual hits (right) and misses (left) across nine electrode sites, arranged from anterior to posterior. Each point and the number above it indicate the mean difference across participants. Error bars and the interval estimate below indicate 95% bootstrapped CIs around the mean difference. Cohen's d_z effect size estimates are reported to the left/right of center for each electrode, with position reflecting the direction of the effect. Associated distributions of differences and topographic representations of mean differences are also plotted for each condition. ***B***, Difference in unadjusted alpha power before auditory (left) and visual (right) hits and misses. ***C***, Difference in alpha power after adjustment before auditory versus visual hits (right) and misses (left). ***D***, Difference in adjusted alpha power before auditory (left) and visual (right) hits versus misses.

for misses over occipital electrode sites), consistent with the appearance in Figure 2*A* that averaged spectra for visual misses tend to occupy an intermediate position between auditory hits/misses and visual hits. With respect to the speaker fault, the posterior amplification of the alpha signal during auditory relative to visual attention appeared more pronounced in those who did not experience the fault (d_z = 0.66–0.82 for $\text{hit}_{\text{auditory-visual}}$ over the posterior row, compared with $\text{hit}_{\text{auditory-visual}}$ d_z values of 0.43–0.53 for those experiencing the speaker fault).

Although posterior alpha power tended to increase when attention was directed to auditory information, this increase did not have an obvious effect on performance. Contrasts of unadjusted power preceding hits versus misses indicate little association between power and performance in this sample, consistent with the negative/null reports from the auditory literature (e.g., Ng et al., 2012; Fig. 4*B*, left). Over posterior electrodes, at the same locations at which the difference between auditory and visual hits was maximal, effect sizes for the difference between auditory hits and misses ranged from 0.17 (Oz) to 0.31 (O1/Contra; note that these effects were exaggerated by the presence of an influential outlier). That is, there was no indication in this sample that the change in posterior alpha amplitude associated with attending to auditory relative to visual information bore a relation to auditory detection in the absence of concurrent or expected visual input.

In contrast, when attending to visual information, unadjusted alpha power preceding hits was consistently reduced relative to alpha power preceding misses, in accord with the broader literature (Fig. 4*B*, right). The most pronounced and consistent differences emerged over posterior electrodes, with effect sizes ranging from $d_z = 0.53$ to 0.76 over the posterior row.

After aperiodic correction

After aperiodic correction, differences in alpha power between auditory and visual tasks were slightly reduced overall and similar in magnitude for $\text{hit}_{\text{auditory-visual}}$ and $\text{miss}_{\text{auditory-visual}}$ contrasts (d_z values of 0.46–0.55 for hits and 0.42–0.50 for misses over the posterior row; Fig. 4*A*). This reduction seems primarily due to the effect of adjustment on visual hits.

The effects of adjustment on hit/miss contrasts were more pronounced (Fig. 4*D*). In the visual domain, the effect of adjustment was generally to reduce the difference between hits and misses, although differences in adjusted power between hits and misses did still tend, on average, to skew negative toward the posterior row (d_z values ranging from 0.38–0.70, compared with 0.53–0.76 before adjustment; Fig. 4*B*, *D*). At central and parietal electrode locations, effects that might previously have appeared ambiguous (in the $d_z = 0.15$–0.35 range) were generally reduced to near zero. Over the posterior, adjustment resulted in smaller effect sizes over contralateral (reduced from $d_z = 0.53$ to 0.38) and central (reduced from $d_z = 0.71$ to 0.55) electrode sites, and a relatively sustained effect over the ipsilateral location (reduced from $d_z = 0.76$ to 0.70). These results are compatible with the suggestion that some of the robust alpha effects reported in the literature (i.e., with respect to visual detection) may be better thought of as combination of alpha and broadband spectral shifts.

In the auditory domain, differences after adjustment were, if anything, slightly amplified occipitally relative to the unadjusted alpha difference and in the same direction as $\text{visual}_{\text{hit-miss}}$ contrasts (i.e., lower power for auditory hits relative to misses; d_z values ranging from 0.29 to 0.34 over the posterior row; note however that the confidence intervals around these differences still generally include zero; Fig. 4*D*).

Overall, the posterior changes in offset/exponent associated with visual detection appear as large and consistent across participants as changes in unadjusted alpha power (or larger) and likely to account for a portion of the visual hit/miss effect in the unadjusted data. That is, the established difference in alpha power that is often reported before visual hits and misses is probably best thought of as a combination of narrowband alpha and broadband shifts in signal amplitude. More broadly, differences in the parameter estimates associated with the aperiodic component of the prestimulus signal appear to differentiate visual hits from all other categories (auditory hits/misses and visual misses) for which the spectra over posterior electrodes were otherwise quite similar. The topography of the aperiodic effects suggests an occipital (visual) locus, and the direction of the effects (flatter slope and reduced offset for visual hits) is consistent with the observations of Gao et al. (2017) that spectral shifts toward flatter slopes and reduced power at lower frequencies tend to indicate a shift toward relative excitation. That is, visual hits may still be preceded by a relative increase in local excitation, but that excitation seems to manifest here both as a change in the aperiodic component of the spectrum and a change in alpha power.

Algorithmic performance with simulated spectra

Although Donoghue et al., (2020a) have done extensive testing and validation of the spectral parameterization procedure used in this article, in light of the results above, it may be useful to demonstrate the validity of the procedure for the current situation. To that end, the following simulations were conducted.

First, the degree to which the algorithm accurately recovers power, exponent, and offset was evaluated in synthetic spectra spanning the range of values observed in our data (Fig. 2*C*–*F*). Each spectrum was generated as the sum in linear space of an aperiodic component (see above, Spectral parameterization, for the formula), a single Gaussian component (alpha), and a small amount of white noise (i.e., noise present to an equal extent at all frequencies). Five simulated offset values were selected to span the range from 0 to 1.75, five exponent values were selected to span the range from 0.75 to 2.0, and five peak alpha power values were selected to span the range from 0.05 to 14. Spectra were generated for all 125 combinations of offset, exponent, and peak alpha power, assuming an alpha peak frequency of 10.25 Hz and a bandwidth of 3.59 Hz (based on the estimated average alpha bandwidth at electrode Oz for participants in this study). The simulated frequency range was 2–50 Hz, with a resolution of 0.5 Hz and a white noise level of 0.005. These spectra were decomposed identically to the data reported above, and the differences between resulting parameter estimates and original values (error) are presented in Figure 5*A*.

The correspondence between simulated and estimated values was very nearly 1–1 (see also Donoghue et al., 2020a). Generally, the algorithm tended to slightly underestimate power ($M_{error} = -0.04$, SD = 0.07) and slightly overestimate offset ($M_{error} = 0.04$, $SD = 0.06$) and exponent ($M_{error} = 0.02$, SD = 0.04). These errors were not systematically related to changes in offset, exponent, or alpha power.

Given the tendency of the algorithm to produce a bias that could have an impact on the results reported above, we also evaluated how the algorithm performed in synthetic situations for which true alpha band effects of varying magnitudes were present. Spectra were simulated as follows: Four effect sizes (Cohen's d_z) were selected spanning a range from 0.35 to 1.0 (0.35, 0.5, 0.85, and 1.0). For each effect size, hit and miss spectra were generated for 27 synthetic participants over a frequency range of 2–50 Hz, with a frequency resolution of 0.5 and a minimal white noise level of 0.005 (mimicking the data presented in Figs. 2 and 4). Unless otherwise specified, the values described below were based on means and SDs recorded at electrode Oz (Fig. 2).

Aperiodic values were simulated assuming no difference between hits/misses. Exponent values for each participant and hit/miss bin were drawn from a normal distribution with a mean of 1.25 and an SD of 0.34. Offset values were drawn from a normal distribution with a mean of 1.10 and an SD of 0.38.

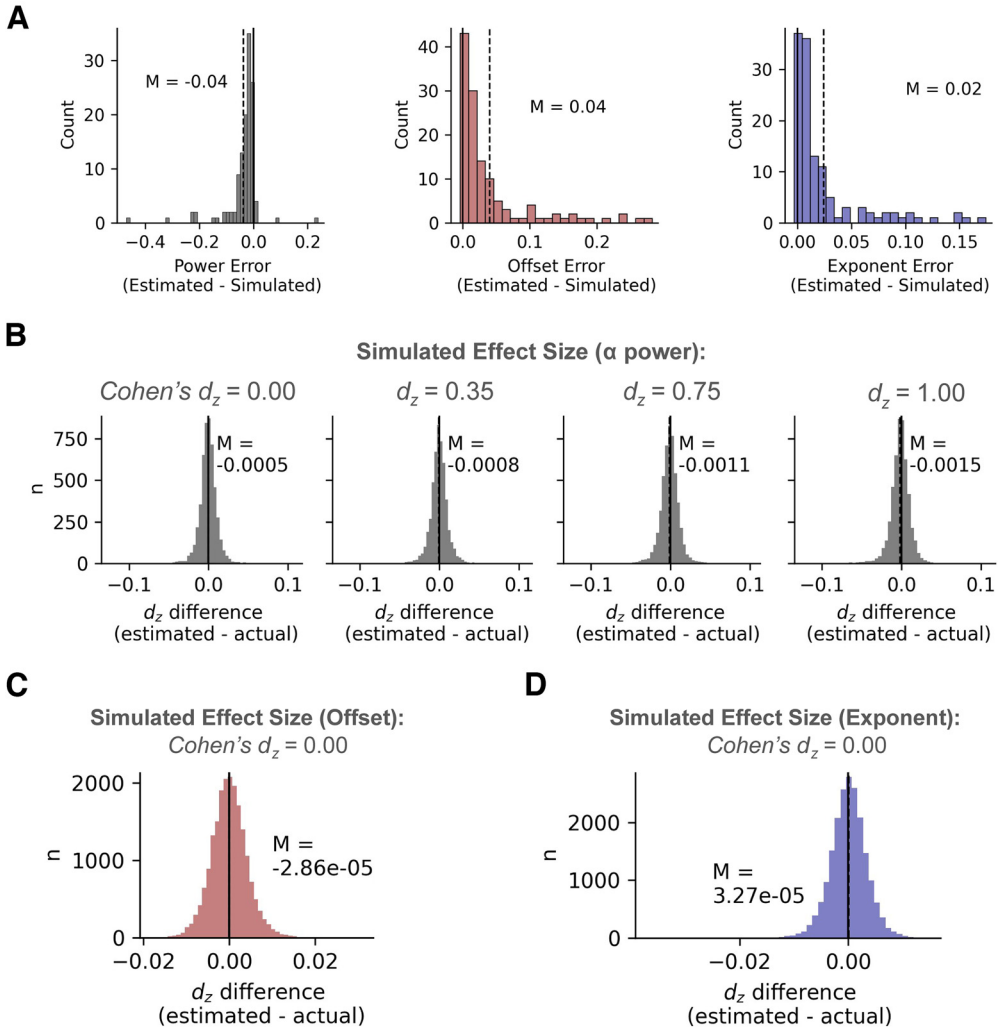

Figure 5. ***A***, Plots of error (estimated minus simulated) in measurement of power (left), offset (middle), and exponent (right) for 125 simulated spectra spanning the range of values recorded in the human data. Each plot contains a vertical reference line at zero and a dashed line indicating mean error. ***B***, Difference between actual (simulated) and estimated effect size (Cohen's d_z) for various sizes of oscillatory alpha-band effect. Each plot is constructed from 5000 simulated samples. Each plot contains a solid vertical reference line at zero and a dashed line indicating mean error. ***C***, ***D***, Difference between simulated effect size ($d_z = 0$) and measured effect size for offset (***C***) and exponent (***D***) in the same data in which oscillatory effects were simulated. Solid reference lines are plotted at zero, and dashed lines indicate average error in d_z.

Alpha power values were simulated for hits and misses assuming the selected effect size. First, initial peak power values were generated for each pseudoparticipant by drawing from a normal distribution with a mean of 2.2 and an SD of 2.65. In addition, 27 mean differences in alpha power were drawn from a normal distribution with a mean derived from the selected effect size and an SD of 0.48 ($M_{diff} = d_z * sd_{diff}$). Hit and miss distributions were created by taking each participant's initial power level and subtracting (for hits) or adding (for misses) half of each participant's mean difference value. Alpha peak frequency was set at 10.25 Hz, and bandwidth was set at 3.59 Hz.

Spectra were generated by taking the sum in linear space of Gaussian (alpha band), aperiodic, and white noise components. Spectra were then decomposed and alpha power, offset, and exponent were computed identically to the manner described for the data above. The effect size of the difference in alpha power for hits versus misses was computed both for the simulated (ground truth) values and their derived estimates. Simulated and estimated d_z values were subtracted to obtain estimates of error in measurement.

Simulations were repeated 5000 times with different random draws for each of the four effect sizes to create the distributions of error in effect size estimation presented in Figure 5*B*. As can be seen in the figure, across a range of effect sizes, the average error in estimation was negligible (~0.001 or less; i.e., if the true alpha power-related effect size was $d_z = 0.75$, the measured effect size would be, on average, $d_z = 0.749$). The algorithm recovers true oscillatory effects quite well when present, and the differences between unadjusted (e.g., $d_z = 0.71$ for electrode Oz) and adjusted ($d_z = 0.55$) alpha-power-related effects observed in the visual data in this article are beyond what could reasonably be attributed to bias in the algorithm.

In addition, the algorithm was not prone to inflating effect sizes associated with offset or exponent. In these simulations, the maximum absolute error in effect size (where the ground truth was a d_z of 0.00 for both offset and exponent) across all 20,000 simulations was 0.032 for offset and 0.015 for exponent (Fig. 5*C*, *D*).

Single-trial analyses

To supplement the analyses above, spectra for single trials were also examined. For visualization, we present the signal decomposed in the conventional manner in which alpha power quantiles are generated from the unadjusted spectra,

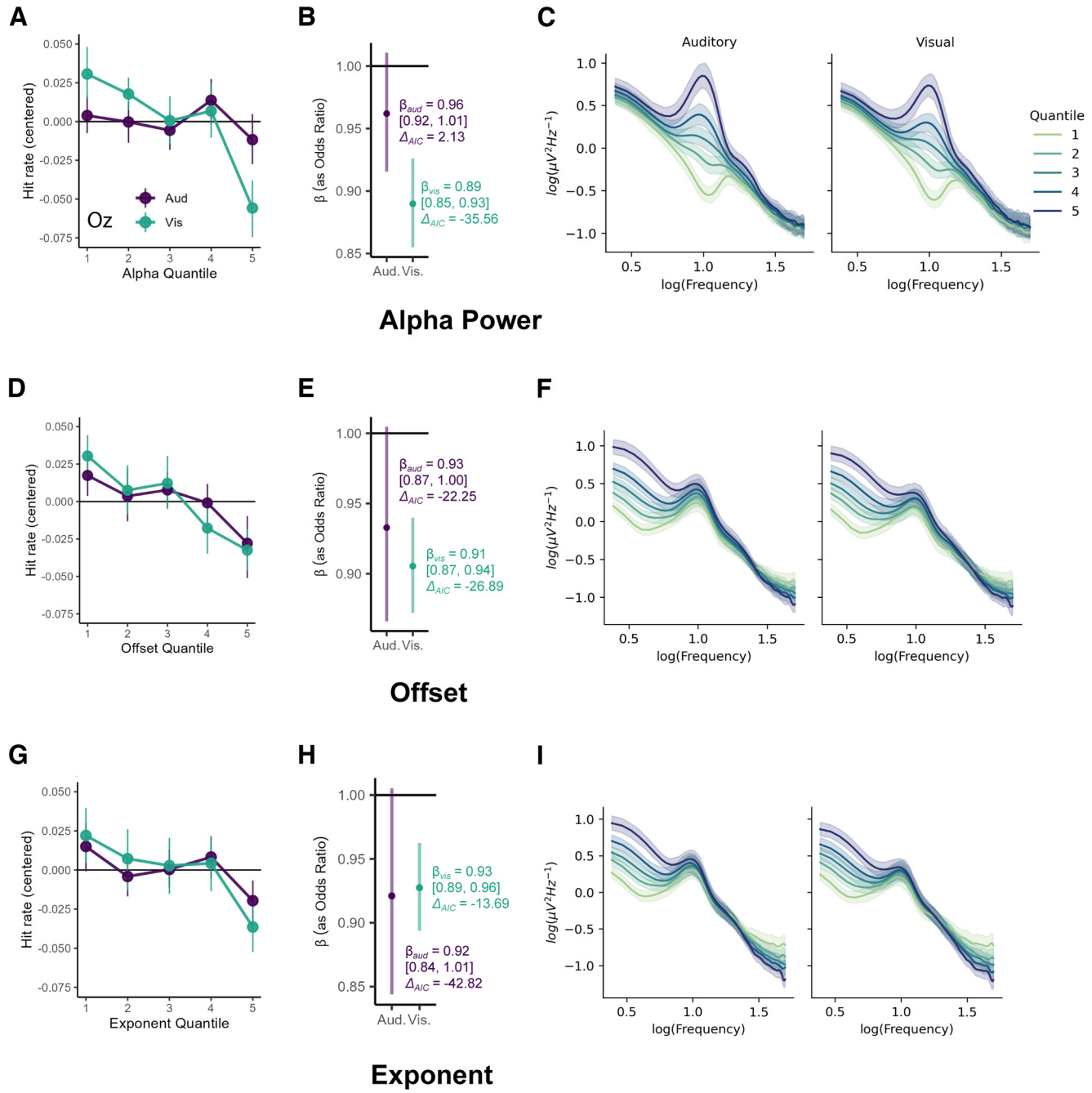

Figure 6. ***A***, Hit rates (centered for each individual/task) as a function of alpha power quantile for electrode Oz. Error bars indicate 95% bootstrapped CIs around the mean. ***B***, Fixed effects estimates for unadjusted alpha power split by task (Aud./Vis.) for channel Oz. Fixed effects are reported in terms of the relation between predictor and odds ratio. Odds ratios greater than or less than one indicate a negative or positive relation, respectively, between power and odds of a hit. Odds ratios of one are equivocal. Points and beta values indicate fixed effects. Error bars and interval estimates indicate 95% CIs surrounding fixed effects. Change in AIC is reported relative to the null model. Negative Δ AIC values indicate improvements in fit. ***C***, Averaged PSDs associated with the alpha quantiles plotted in ***A*** in log–log space for ease of viewing. Ribbons indicate 95% bootstrapped CIs. ***D–F***, The same plots as in ***A–C*** but with quantiles split by offset estimate. ***G–I***, The same plots as in ***A–C*** but with quantiles split by exponent.

and hit rates are plotted as a function of quantile (for a representative electrode; Fig. 6*A*). Given the association between offset/exponent and visual hits/misses in the averaged data, we also present quantile splits based on single-trial estimates of offset and exponent (Fig. 6*C*, *E*).

To provide a trial-level estimate of the relation between alpha band and aperiodic components of the signal and behavior, we decomposed single-trial spectra to obtain estimates of unadjusted alpha power, offset, and exponent, and used these as predictors of hit likelihood in mixed-effects logistic regression analyses (with separate models for auditory and visual data). First, for each combination of electrode and task modality, null (baseline) models were generated with a random intercept term to account for participant-level variation in overall performance. Models containing offset, exponent, and unadjusted alpha power as predictors were compared against these null models to evaluate the extent to which each variable separately improved model fit. For all predictors, including random slopes (i.e., allowing slope to vary by individual) improved model fit across most channels beyond that produced by including the fixed effect alone,

particularly for the auditory task. Random slopes were therefore incorporated into all models described here.

As expected, increased posterior alpha power was associated with a marked decline in visual, but not auditory, hit rate. In the visual task, compared with a null model containing only the random effect of participant, a model containing a fixed effect and random slope for unadjusted alpha power resulted in better fits over the posterior row (e.g., ΔAIC of −35.56 at electrode Oz; Fig. 6*B*). The fixed effect of unadjusted alpha power on the odds of a hit was $\beta_{Oz} = 0.89$, 95% CI [0.85, 0.93]. That is, an increase of one SD in posterior prestimulus alpha power was associated with, approximately, a 10% reduction in the odds of a hit. For the auditory task, adding unadjusted alpha power to the model had little effect on fit over posterior electrode sites [indicating little association between unadjusted alpha power and performance; $\beta_{Oz} = 0.96$, 95% CI (0.92, 1.01), $\Delta_{AIC} = 2.13$].

Increases in aperiodic offset and exponent were similarly associated with a marked decline in hit rates in the visual data. (Note that in the auditory data, the apparent negative relation between offset/exponent and hit rate is largely the result of a single outlying participant, also visible in Fig. 2*D*,*E*.) Models containing fixed effects and random slopes for offset performed substantially better than null models over posterior electrodes in the visual task (e.g., ΔAIC of −26.89 at electrode Oz), as did models containing fixed effects and random slopes for exponent (ΔAIC of −13.69 at electrode Oz). The fixed effects of offset and exponent were similar in magnitude to the effect of unadjusted alpha power [offset, $\beta_{Oz} = 0.91$, 95% CI (0.87, 0.94); exponent, $\beta_{Oz} = 0.93$, 95% CI (0.89, 0.96)]. In the auditory task, models containing offset and/or exponent as a predictor resulted in substantial improvements in fit across all electrodes, with fixed effects generally in the same direction as in vision. However, interval estimates surrounding auditory fixed effects indicated substantial variability compared with their visual counterparts (Fig. 6*E*, *H*).

We also examined the spectra associated with each quantile (Fig. 6*C*, *F*, *I*; Iemi et al., 2019). When data were split by alpha power (Fig. 6*C*), spectra showed not only the expected α gradation but also a broadband shift associated with that gradation, present during both audition and vision, consistent with prior reports (Iemi et al., 2019). Similarly, when data were split by offset/exponent (Fig. 6*F*, *I*), spectra showed not only a broadband gradation/rotation, but also a gradation in unadjusted alpha power. Within-participant and across modalities, the association between unadjusted alpha power and offset was small but uniformly positive (average $\rho_{Spearman} = 0.19$, SD = 0.07 at electrode Oz). The association between alpha power and exponent was similarly small, and positive for all but one participant in each modality (average $\rho_{Spearman} = 0.11$, SD = 0.07 at electrode Oz; in addition, and unsurprisingly, there was a strong positive association between exponent and offset, average $\rho_{Spearman} = 0.95$, SD = 0.01 at electrode Oz). After aperiodic adjustment, associations between single-trial alpha power and offset/exponent estimates were reduced to near zero (average $\rho_{Spearman} = 0.05$ and 0.02 for offset and exponent, respectively, at electrode Oz).

These results largely corroborate the observations already discussed (see above, Results). The association between prestimulus alpha power and visual detection appears to be paralleled, and perhaps partially accounted for, by shifts in the aperiodic component of the signal. In addition, although increased power in the alpha band was associated with changes in offset and exponent across both audition and vision, there was no indication of a consistent association between parietal/occipital changes in any of these components and performance when participants were engaged in auditory detection.

Discussion

The initial purpose of this experiment was to integrate observations regarding alpha power dynamics from intersensory contexts with similar observations from the auditory/visual detection literature, with the goal of developing a better understanding of the conditions under which patterns of parieto-occipital alpha amplification/suppression relate to detection or awareness of threshold stimuli. What we have found is that these dynamics are best described not merely as alpha-related but rather as a combination of narrowband alpha and broadband aperiodic shifts.

With respect to the auditory data, posterior alpha power exhibited the typical increase during auditory relative to visual attention, although this effect was slightly reduced following aperiodic adjustment. This attention-related effect was not paralleled by any consistent effects associated with auditory detection (either preadjustment or postadjustment), a set of results largely consistent with existing unimodal auditory reports (Ng et al., 2012; van Diepen and Mazaheri, 2017); although systematic manipulation of experimental context may be necessary to reconcile this with some elements of the auditory literature). There were no consistent links between aperiodic components of the signal and auditory attention or detection, but this result should be taken in the context of the posterior bias of the electrode array.

The visual results are more striking. The examination of visual detection was initially intended to provide a baseline for comparison with the auditory data, as well as a manipulation check to ensure that we were able to reproduce an alpha-behavior relation that has been reported and interrogated at length by others (Ergenoglu et al., 2004; van Dijk et al., 2008; Romei et al., 2008; Busch et al., 2009; Mathewson et al., 2009; Busch and VanRullen, 2010; Boncompte et al., 2016; Limbach and Corballis, 2016; Benwell et al., 2017; Iemi et al., 2017; Samaha et al., 2017, 2020). What we have found is that the relation between prestimulus alpha power and visual hit rate is, at least in these data, at least partially attributable to shifts in the broadband component of the signal. When the data are parceled into aperiodic and periodic components, the size of narrowband alpha-related effects is generally reduced and paralleled by sizeable changes in aperiodic offset and exponent.

These observations are consistent with a number of previous reports that suggest that links between oscillatory power and behavior may be exaggerated by virtue of being confounded with shifts in the aperiodic signal (Iemi et al., 2019; Donoghue et al., 2020a,b; Ouyang et al., 2020; Waschke et al., 2021). For example, Iemi et al. (2019) describe the impact of prestimulus broadband activity on measurement of alpha-band oscillatory activity and, in the context of examining the relation between oscillatory power and amplitude of subsequent event-related responses, were the first to identify and describe the extent to which broadband spectral shifts contaminate the standard quantile-split approach that is often used to relate alpha power to behavior (an observation that is reproduced here). Ouyang et al. (2020) illustrate that when appropriately separated, the aperiodic component of the signal, but not alpha power, predicts cognitive processing speed (a relation that would have been attributed to alpha-band activity using conventional methods of decomposition).

Perhaps the most relevant recent report is that of Waschke et al. (2021), who demonstrate that the spectral exponent can change systematically in response to attentional modulation. Specifically, they observe a flattening of spectral exponent (thought to indicate a shift toward relative excitation) over occipital regions when attention is directed to visual versus auditory information. (And vice versa, when attention is directed toward auditory over visual information, a relative flattening is observed at frontocentral sites.) Although here our coverage of frontocentral regions is too limited to reproduce these results in full, our observation of flattened posterior spectra during visual relative to auditory attention is consistent with their results. (Podvalny et al. 2015 provides a related example of spectral flattening in visual cortex related to visual stimulation.)

Our observation of flatter posterior spectra associated with visual hits is also broadly consistent with another piece of evidence provided by Waschke et al. (2021). In brief, the hypothesis has been put forward that changes 1/f-like activity in the EEG power spectrum reflect changes in excitation–inhibition balance, with observable shifts in slope/offset resulting from differences in the relative speeds of activity at faster excitatory and slower inhibitory synapses (Gao et al., 2017). Increases in relatively slower inhibitory activity, for example, may result in larger offsets and steeper negative slopes due to relative increases in power at lower frequencies. Waschke et al. (2021) probed this hypothesis by examining the response of the human spectral exponent to anesthesia and found, among other observations, increases in steepness linked to inhibitory propofol administration (and reductions in steepness linked to ketamine administration). In our results, over occipital regions, flatter slopes and broad reductions in low-frequency power were consistently linked to visual hits. The direction of these effects is consistent with the notion that flatter slopes (reduced exponent) and reductions in power broadly at lower frequencies (reduced offset) signal shifts in excitation–inhibition balance toward relative excitation.

The implications of these results are at least twofold. On the one hand, as mentioned, if these data are representative of the broader literature, existing estimates of alpha–behavior relationships are likely exaggerated. The extent of this exaggeration remains to be seen, given substantial inter-study variation in protocol, and reanalysis of existing datasets might be required to develop converging estimates of the relative strength of aperiodic/periodic effects. On the other hand, the relation between aperiodic offset/exponent and visual awareness appears relatively strong and consistent across individuals. It may be that aperiodic effects, which are currently undercharacterized, provide an as or more useful indicator of fluctuations in attentional state in scalp-level recordings than adjusted or unadjusted alpha power dynamics.

Here, we should note a minor dissociation in our data between effects linked to modality-specific attention and those linked to visual detection. In both cases, adjusting for the aperiodic component of the signal reduced the size of alpha-power-related effects. However, only in the case of visual performance was there a substantial corresponding effect related to aperiodic offset/exponent. (The relation between aperiodic offset and attention to modality was not null, but it was also not close to the effect size observed in relation to visual hits/misses.) It could be that more substantial changes in the aperiodic component of the signal would be observed across modalities in within-session comparisons (Waschke et al., 2021). In fact, assuming broadband shifts largely reflect changes in excitation–inhibition balance, given that anticipatory increases in baseline firing rates are one of the most well-known effects of attention on neural activity (Luck et al., 1997) and that attention to a sensory modality is typically accompanied by patterns of enhanced/reduced activity in regions of primary and association cortex linked to attended/unattended modalities (Kawashima et al., 1995; Johnson and Zatorre, 2005, 2006; Langner et al., 2011), it would not be surprising to see these changes reflected in the scalp-level broadband signal.

The intent of this work is not to claim that there is no relation between alpha circuit activity and subjective awareness of threshold visual information, but merely that at least in the scalp-recorded signal, the effect size may be smaller than it has initially appeared, and that changes in parameters associated with the aperiodic component of the signal may be as or more consistently linked to performance than changes in alpha power per se. Taken together with a recent report suggesting that an association between narrowband alpha amplitude and both poststimulus excitation and behavior can be observed at the intracranial level even after adjusting for aperiodic 1/f-like activity (Iemi et al., 2022), this may indicate that although periodic effects persist in the brain, they are simply more difficult to record at the scalp level than the literature would lead one to expect.

Across the relatively extensive alpha literature, systematic reports separating aperiodic and periodic variation in the signal are still quite limited, such that gauging the relative contributions of these two dimensions of variation is something of a challenge. Given that the data here were collected with a limited electrode array in the context of largely exploratory analyses, these observations are certainly preliminary. It will take additional experimentation and/or independent reanalysis of existing data to confirm, contradict, or narrow our expectations regarding the relations between attention, alpha-band activity, and broadband spectral shifts. It is our hope that this work will encourage the re-examination of a rich body of data that already exists, with the aim of obtaining a more precise understanding of if/when scalp-recorded alpha signals are truly modulated in relation to attention/perception and when the alpha signal is better thought of as a carrier for broadband effects.

References

Adrian ED (1944) Brain rhythms. Nature 153:360–362.

Akaike H (1974) A new look at the statistical model identification. IEEE Trans Automat Contr 19:716–723.

Bates D, Mächler M, Bolker B, Walker S (2015) Fitting linear mixed-effects models using lme4. J Stat Softw 67:1–48.

Bazanova OM, Vernon D (2014) Interpreting EEG alpha activity. Neurosci Biobehav Rev 44:94–110.

Benwell CSY, Tagliabue CF, Veniero D, Cecere R, Savazzi S, Thut G (2017) Prestimulus EEG power predicts conscious awareness but not objective visual performance. eNeuro 4:ENEURO.0182-17.2017.

Bernasconi F, Manuel AL, Murray MM, Spierer L (2011) Pre-stimulus beta oscillations within left posterior sylvian regions impact auditory temporal order judgment accuracy. Int J Psychophysiol 79:244–248.

Bollimunta A, Chen Y, Schroeder CE, Ding M (2008) Neuronal mechanisms of cortical alpha oscillations in awake-behaving macaques. J Neurosci 28:9976–9988.

Boncompte G, Villena-González M, Cosmelli D, López V (2016) Spontaneous alpha power lateralization predicts detection performance in an un-cued signal detection task. PLoS One 11:e0160347.

Burnham KP, Anderson DR, Huyvaert KP (2011) AIC model selection and multimodel inference in behavioral ecology: some background, observations, and comparisons. Behav Ecol Sociobiol 65:23–35.

Busch NA, VanRullen R (2010) Spontaneous EEG oscillations reveal periodic sampling of visual attention. Proc Natl Acad Sci U S A 107:16048–16053.

Busch NA, Dubois J, VanRullen R (2009) The phase of ongoing EEG oscillations predicts visual perception. J Neurosci 29:7869–7876.

Donoghue T, Haller M, Peterson EJ, Varma P, Sebastian P, Gao R, Noto T, Lara AH, Wallis JD, Knight RT, Shestyuk A, Voytek B (2020a) Parameterizing neural power spectra into periodic and aperiodic components. Nat Neurosci 23:1655–1665.

Donoghue T, Dominguez J, Voytek B (2020b) Electrophysiological frequency band ratio measures conflate periodic and aperiodic neural activity. eNeuro 7:ENEURO.0192-20.2020.

ElShafei HA, Bouet R, Bertrand O, Bidet-Caulet A (2018) Two sides of the same coin: distinct sub-bands in the α rhythm reflect facilitation and suppression mechanisms during auditory anticipatory attention. eNeuro 5: ENEURO.0141-18.2018.

Ergenoglu T, Demiralp T, Bayraktaroglu Z, Ergen M, Beydagi H, Uresin Y (2004) Alpha rhythm of the EEG modulates visual detection performance in humans. Brain Res Cogn Brain Res 20:376–383.

Foxe JJ, Simpson GV, Ahlfors SP (1998) Parieto-occipital approximately 10 Hz activity reflects anticipatory state of visual attention mechanisms. Neuroreport 9:3929–3933.

Fu K-MG, Foxe JJ, Murray MM, Higgins BA, Javitt DC, Schroeder CE (2001) Attention-dependent suppression of distracter visual input can be cross-modally cued as indexed by anticipatory parieto–occipital alpha-band oscillations. Brain Res Cogn Brain Res 12:145–152.

Gao R, Peterson EJ, Voytek B (2017) Inferring synaptic excitation/inhibition balance from field potentials. Neuroimage 158:70–78.

Gramfort A, Luessi M, Larson E, Engemann D, Strohmeier D, Brodbeck C, Goj R, Jas M, Brooks T, Parkkonen L, Hämäläinen M (2013) MEG and EEG data analysis with MNE-Python. Front Neurosci 7:267.

Gratton G, Coles MGH, Donchin E (1983) A new method for off-line removal of ocular artifact. Electroencephalogr Clin Neurophysiol 55:468–484.

Gyurkovics M, Clements GM, Low KA, Fabiani M, Gratton G (2022) Stimulus-induced changes in 1/f-like background activity in EEG. J Neurosci 42:7144–7151.

Haegens S, Nácher V, Luna R, Romo R, Jensen O (2011) α-Oscillations in the monkey sensorimotor network influence discrimination performance by rhythmical inhibition of neuronal spiking. Proc Natl Acad Sci U S A 108:19377–19382.

Haegens S, Luther L, Jensen O (2012) Somatosensory anticipatory alpha activity increases to suppress distracting input. J Cogn Neurosci 24:677–685.

Haegens S, Cousijn H, Wallis G, Harrison PJ, Nobre AC (2014) Inter- and intra-individual variability in alpha peak frequency. Neuroimage 92:46–55.

Hansen NE, Harel A, Iyer N, Simpson BD, Wisniewski MG (2019) Pre-stimulus brain state predicts auditory pattern identification accuracy. NeuroImage 199:512–520.

Iemi L, Chaumon M, Crouzet SM, Busch NA (2017) Spontaneous neural oscillations bias perception by modulating baseline excitability. J Neurosci 37:807–819.

Iemi L, Busch NA, Laudini A, Haegens S, Samaha J, Villringer A, Nikulin VV (2019) Multiple mechanisms link prestimulus neural oscillations to sensory responses. Elife 8:e43620.

Iemi L, Gwilliams L, Samaha J, Auksztulewicz R, Cycowicz YM, King J-R, Nikulin VV, Thesen T, Doyle W, Devinsky O, Schroeder CE, Melloni L, Haegens S (2022) Ongoing neural oscillations influence behavior and sensory representations by suppressing neuronal excitability. Neuroimage 247:118746.

Johnson JA, Zatorre RJ (2005) Attention to simultaneous unrelated auditory and visual events: behavioral and neural correlates. Cereb Cortex 15:1609–1620.

Johnson JA, Zatorre RJ (2006) Neural substrates for dividing and focusing attention between simultaneous auditory and visual events. Neuroimage 31:1673–1681.

Kawashima R, O'Sullivan BT, Roland PE (1995) Positron-emission tomography studies of cross-modality inhibition in selective attentional tasks: closing the "mind's eye". Proc Natl Acad Sci U S A 92:5969–5972.

Kayser SJ, McNair SW, Kayser C (2016) Prestimulus influences on auditory perception from sensory representations and decision processes. Proc Natl Acad Sci U S A 113:4842–4847.

Langner R, Kellermann T, Boers F, Sturm W, Willmes K, Eickhoff SB (2011) Modality-specific perceptual expectations selectively modulate baseline activity in auditory, somatosensory, and visual cortices. Cereb Cortex 21:2850–2862.

Limbach K, Corballis PM (2016) Prestimulus alpha power influences response criterion in a detection task: prestimulus alpha power influences response. Psychophysiology 53:1154–1164.

Luck SJ, Chelazzi L, Hillyard SA, Desimone R (1997) Neural mechanisms of spatial selective attention in areas V1, V2, and V4 of macaque visual cortex. J Neurophysiol 77:24–42.

Makeig S, Inlow M (1993) Lapse in alertness: coherence of fluctuations in performance and EEG spectrum. Electroencephalogr Clin Neurophysiol 86:23–35.

Mathewson KE, Gratton G, Fabiani M, Beck DM, Ro T (2009) To see or not to see: prestimulus α phase predicts visual awareness. J Neurosci 29:2725–2732.

Mazaheri A, van Schouwenburg MR, Dimitrijevic A, Denys D, Cools R, Jensen O (2014) Region-specific modulations in oscillatory alpha activity serve to facilitate processing in the visual and auditory modalities. Neuroimage 87:356–362.

Miller KJ, Sorensen LB, Ojemann JG, den Nijs M (2009) Power-law scaling in the brain surface electric potential. PLOS Comput Biol 5: e1000609.

Ng BSW, Schroeder T, Kayser C (2012) A precluding but not ensuring role of entrained low-frequency oscillations for auditory perception. J Neurosci 32:12268–12276.

Ouyang G, Hildebrandt A, Schmitz F, Herrmann CS (2020) Decomposing alpha and 1/f brain activities reveals their differential associations with cognitive processing speed. Neuroimage 205:116304.

Peirce J, Gray JR, Simpson S, MacAskill M, Höchenberger R, Sogo H, Kastman E, Lindeløv JK (2019) PsychoPy2: experiments in behavior made easy. Behav Res Methods 51:195–203.

Podvalny E, Noy N, Harel M, Bickel S, Chechik G, Schroeder CE, Mehta AD, Tsodyks M, Malach R (2015) A unifying principle underlying the extracellular field potential spectral responses in the human cortex. J Neurophysiol 114:505–519.

Romei V, Brodbeck V, Michel C, Amedi A, Pascual-Leone A, Thut G (2008) Spontaneous fluctuations in posterior α-band EEG activity reflect variability in excitability of human visual areas. Cereb Cortex 18:2010–2018.

Samaha J, Iemi L, Postle BR (2017) Prestimulus alpha-band power biases visual discrimination confidence, but not accuracy. Conscious Cogn 54:47–55.

Samaha J, Iemi L, Haegens S, Busch NA (2020) Spontaneous brain oscillations and perceptual decision-making. Trends Cogn Sci 24:639–653.

Strauß A, Henry MJ, Scharinger M, Obleser J (2015) Alpha phase determines successful lexical decision in noise. J Neurosci 35:3256–3262.

Thut G, Nietzel A, Brandt SA, Pascual-Leone A (2006) A-band electroencephalographic activity over occipital cortex indexes visuospatial attention bias and predicts visual target detection. J Neurosci 26:9494–9502.

van Diepen RM, Mazaheri A (2017) Cross-sensory modulation of alpha oscillatory activity: suppression, idling, and default resource allocation. Eur J Neurosci 45:1431–1438.

van Dijk H, Schoffelen J-M, Oostenveld R, Jensen O (2008) Prestimulus oscillatory activity in the alpha band predicts visual discrimination ability. J Neurosci 28:1816–1823.

Waschke L, Donoghue T, Fiedler L, Smith S, Garrett DD, Voytek B, Obleser J (2021) Modality-specific tracking of attention and sensory statistics in the human electrophysiological spectral exponent. Elife 10:e70068.

Wickham H, et al. (2019) Welcome to the tidyverse. JOSS 4:1686.

Worden MS, Foxe JJ, Wang N, Simpson GV (2000) Anticipatory biasing of visuospatial attention indexed by retinotopically specific α-bank electroencephalography increases over occipital cortex. J Neurosci 20:RC63.